Contribution of Side Resistance and Tip Resistance on the Total Axial Load Capacity of Drilled Shaft Foundations

Conference Paper *in* Electronic Journal of Geotechnical Engineering · April 2013

CITATION
1

READS
76

2 authors:

Masood Hajali
Pure Technologies
25 PUBLICATIONS **9** CITATIONS
SEE PROFILE

Caesar Abishdid
Lebanese American University
31 PUBLICATIONS **65** CITATIONS
SEE PROFILE

EJGE

Contribution of the Side Resistance and Tip Resistance on the Total Axial Load Capacity of Drilled Shaft Foundations

Masood Hajali[1], Caesar Abishdid[2]
1 *Ph.D. Candidate, Dept. of Civil and Environmental Engineering*
Florida International University, Miami, FL 33174 USA
e-mail: mhaja002@fiu.edu
2 *Director of External Programs, College of Engineering and Computing,*
Florida International University, Miami, FL 33174, USA
e-mail: abishdid@fiu.edu

ABSTRACT

The main loads applied on the drilled shafts are axial compressive loads. It is important to know how many percent of the maximum applied load will be shed in side friction and how much will be transferred to the base. Part of the axial load carrying capacity of the drilled shaft is resisted by the soil below the tip of the shaft which is tip resistance and the other part is resisted by the friction developed around the drilled shaft which is side resistance. The axial capacity of the drilled shaft foundation is influenced by the size of the drilled shaft, and soil characteristics. In this study, the effect of the size and soil characteristic will be investigated on the contribution of side resistance and end bearing capacity. Also, the study presents a three-dimensional finite element modeling of a drilled shaft subjected to axial load using ANSYS12. The top displacement and settlement of the drilled shaft are verified with analytical results. The soil profile is considered as Table 1 and for a drilled shaft with 7 ft diameter and 95 ft length the stresses in z-direction are calculated through the length of the shaft. There is a good agrrement between analythical and finite element results in contribution of side resistance and tip resistance for the drilled shaft.

KEYWORDS: Drilled Shaft, Side Resistance, Tip Resistance, Axial Load Capacity, Finite Element Method

INTRODUCTION

Drilled shafts are the most popular of deep foundations, because they have the capability that one single shaft can easily carry the entire load of a large column from a bridge or tall building. Drilled shaft may be an economical alternative to pile foundations because a pile cap is not needed, which not only reduces that expense, but also provides a rough surface in the border of soil and concrete to carry more axial load. Due to the larger construction sizes of drilled shafts, they have excellent axial load carrying capacity.

The condition at the bottom of the excavation can affect the end bearing capacity of the drilled shaft. Also, type of the soil and size of the drilled shaft can affect the frictional resistance. The side resistance and end bearing capacity's equations of the drilled shaft foundation in cohesive and cohesion-less soils are shown here from AASHTO standard [2].

DRILLED SHAFT RESISTANCE

Drilled shafts shall be designed to have adequate axial and structural resistance, tolerable settlements, and tolerable lateral displacement. Nominal axial compression resistance of a single drilled shaft is computed from Equation 1.

The factored resistance of drilled shafts, R_R, shall be taken as:

$$R_R = \phi R_n = \phi_{qp} R_p + \phi_{qs} R_s \tag{1}$$

in which:

$$R_R = q_p A_p \tag{2}$$

$$R_s = \sum q_{si} A_{si} \tag{3}$$

where R_p is nominal shaft tip resistance (kips), R_s is nominal shaft side resistance (kips), ϕ_{qp} is resistance factor for tip resistance specified in table 10.5.5.2.4-1 in AASHTO, ϕ_{qs} is resistance factor for side resistance specified in table 10.5.5.2.4-1 in AASHTO, q_p is unit tip resistance (ksf), q_s is unit side resistance (ksf), A_p is area of shaft tip (ft^2), and A_s is area of shaft side surface (ft^2).

Estimation of Drilled Shaft Resistance in Cohesive Soils

Side Resistance

The nominal unit side resistance, q_s in ksf, for shafts in cohesive soil loaded under un-drained loading conditions by the α-Method shall be taken as:

$$\begin{gathered} q_s = \alpha \ S_u \\ \alpha = 0.55 \quad for \quad \frac{S_u}{P_a} \le 1.5 \\ \alpha = 0.55 - 0.1\left(\frac{S_u}{P_a} - 1.5\right) \quad for \quad 1.5 \le \frac{S_u}{P_a} \le 2.5 \end{gathered} \tag{4}$$

where S_u is un-drained shear strength, α is adhesion factor (dim), P_a is atmospheric pressure (=2.12 ksf)

Tip Resistance

For axially loaded shafts in cohesive soil, the nominal unit tip resistance, q_p, by the total stress method as provided in O'Neill and Reese (1999) [1] shall be taken as:

$$q_p = N_c \ S_u \le 80.0 \tag{5}$$

$$N_c = 6 \ [1 + 0.2(\frac{Z}{D})] \le 9 \tag{6}$$

where D is diameter of drilled shaft (ft), Z is penetration of shaft (ft), S_u is undrained shear strength (ksf).

Estimation of Drilled Shaft Resistance in Cohesion-less Soils

Side Resistance

The nominal unit side resistance is calculated by:

$$q_s = \beta\ \sigma_v' \le 4.0 \qquad for \quad 0.25 \le \beta \le 1.2 \tag{1}$$

in which for sandy soil:

$$\beta = 1.5 - 0.135\sqrt{z} \qquad for \quad N_{60} \ge 15 \tag{8}$$

$$\beta = (\frac{N_{60}}{15})(1.5 - 0.135\sqrt{z}) \qquad for \quad N_{60} < 15 \tag{9}$$

where σ_v' is vertical effective stress at soil layer mid-depth (ksf), β is load transfer coefficient (dim), z is depth below ground, at soil layer mid-depth (ft), and N_{60} is average SPT blow count in the design zone under consideration.

For gravelly sands and gravels:

$$\beta = 2.0 - 0.06(z)^{0.75} \qquad for \quad N_{60} \ge 15 \tag{10}$$

$$\beta = (\frac{N_{60}}{15})(1.5 - 0.135\sqrt{z}) \qquad for \quad N_{60} < 15 \tag{11}$$

Tip Resistance

The nominal tip resistance, q_p in ksf, for drilled shafts in cohesion-less soils by the O'Neill and Reese (1999) [1] method shall be taken as:

$$q_p = 1.2N_{60} \qquad for \quad N_{60} \le 50 \tag{12}$$

where N_{60} is the average SPT blow count in the design zone under consideration

$$q_p = 0.59[N_{60}(\frac{P_a}{\sigma_v'})]^{0.8}\sigma_v' \qquad for \quad N_{60} > 50 \tag{13}$$

P_a is atmospheric pressure (=2.12 ksf), and σ_v' is vertical effective stress at the tip elevation of the shaft (ksf).

ANALYTICAL WORK

A cohesionless (drained) soil profile is considered based on the Standard Penetration Test (SPT) was performed in Phoenix, Arizona soil [6] profile as shown in Table 1.

Table 1: Soil Profile [6]

Depth (ft)	Soil Type	N_{60} (blows/ft)
0-25	Fine to coarse sands	25
25-75	Gravelly sands	42
75-90	Fine to coarse sands	18
90-130	Gravels	49

The total axial resistance versus depth is developed using Equations 1 to 13 for the drilled shafts with different diameters for both cohesive and cohesion-less soils. The soil profile is commonly divided into layers and the depth z is measured to the center of a layer. For each 5 ft layer, vertical effective stress at soil layer mid-depth (ksf) is obtained from Table 1. Load transfer coefficient and unit side resistance is calculated at depth z from Equations 7, 8, and 9 and the side resistance for that layer is obtained by multiplying the unit friction resistance with the perimeter area of the shaft. Figure 1 shows the side resistance versus depth for the drilled shafts with different diameters from 4 feet to 10 feet and length of up to 130 feet.

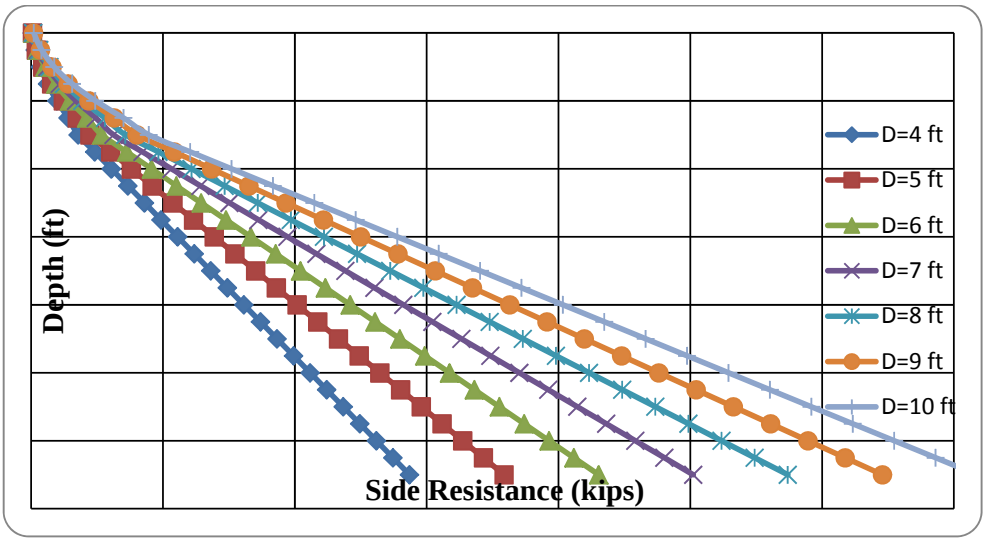

Figure 1: Side Resistance vs. Depth for Different Drilled Shaft Diameters

Also, vertical unit tip resistance is calculated from Equations 12 and the tip resistance for that layer is obtained by multiplying the unit tip resistance with the base area of the drilled shaft. The side diameter and the base diameter for each drilled shaft are considered the same. Figure 2 shows the tip resistance versus depth for the drilled shafts with different diameters.

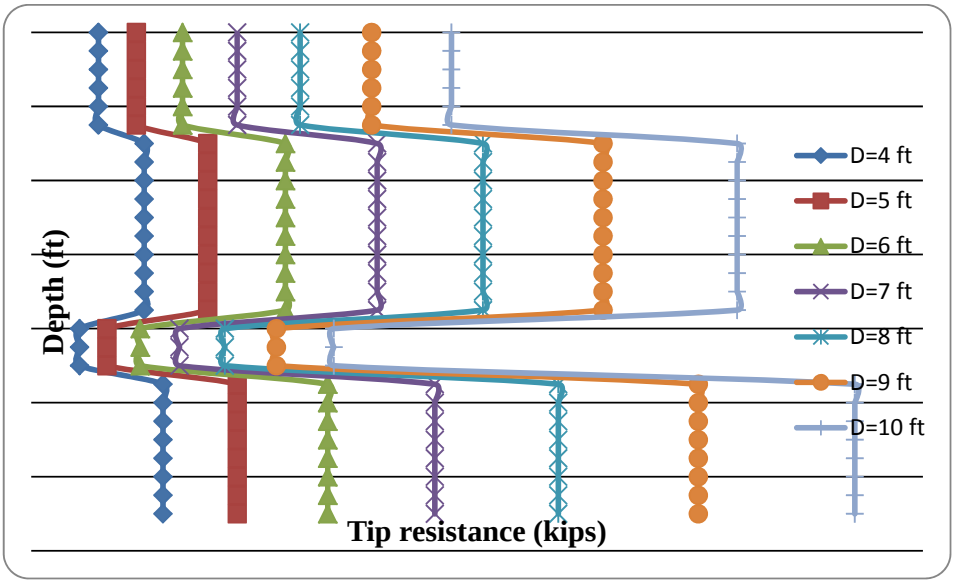

Figure 2: Tip Resistance vs. Depth for Different Drilled Shaft Diameters

Therefore, the total axial resistance of drilled shafts is shaft tip resistance plus shaft side resistance. Figure 3 shows the total axial resistance versus depth for the drilled shafts from 4 ft to 10 ft diameteres.

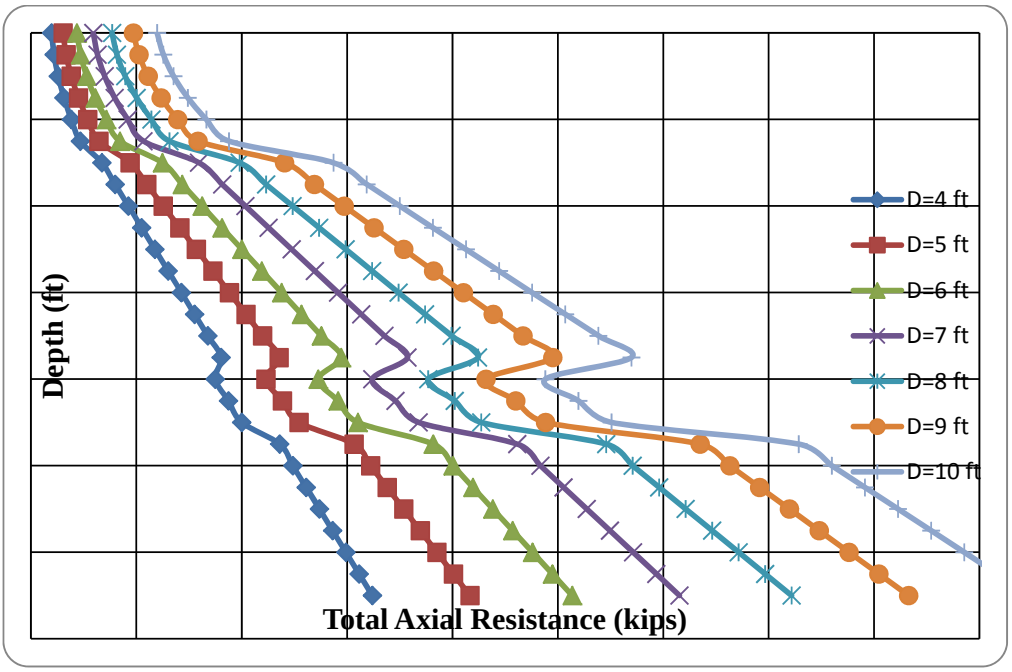

Figure 3: Total Axial Resistance vs. Depth for Different Drilled Shaft Diameters

Figure 4 shows the side resistance percentage of the drilled shafts for different diameters. It can be seen that with increasing in the depth of the drilled shaft side resistance percentage is increased on a second degree polynomial curve.

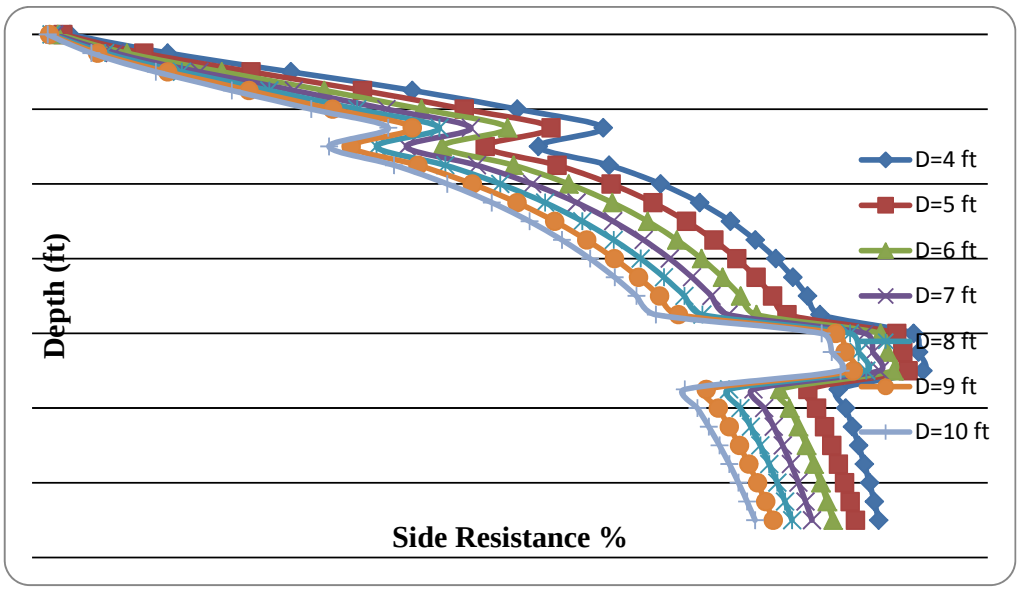

Figure 4: Side Resistance Percentage vs. Depth for Different Drilled Shaft Diameters

FINITE ELEMENT MODEL

Full three-dimensional geometric model is used to represent the soil and drilled shaft as shown in Figure 5. Drilled shaft is analyzed in ANSYS software. The diameter of the drilled shaft is D=7 ft and the length of the drilled shaft is L_1=95 ft. A cylindrical volum is considered as a media for the soil around the drilled shaft with the length and width of 2*L_1 and the diameter of 2*D. This size is selected for the soil volume around the drilled shaft because it has the closest result to the analytical results. The constructed model contains soil, concrete, and reinforcement bars. Four nodes tetrahedral structural solid with rotations is used for soil and eight nodes element is used for concrete as shown in Figure 6. The contact elements are used to connect the nodes between soil and concrete around the drilled shaft for contact and sliding between two surfaces.

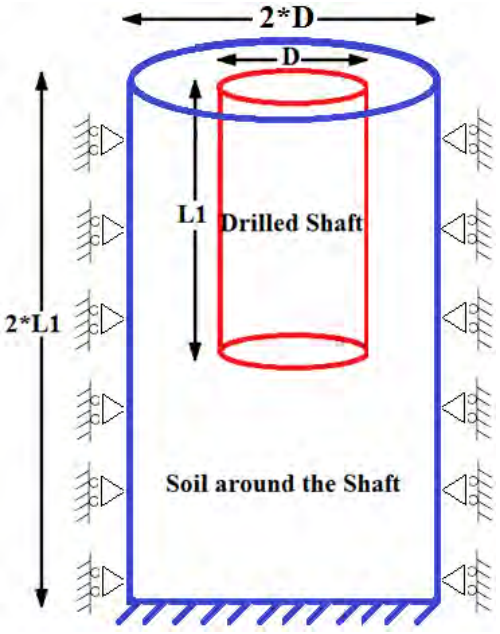

Figure 5: Drilled Shaft Geometry

The mesh size of the drilled shaft part is smaller than the soil region. Total of 13617 nodes and 14802 elements (including 1008 contact elements) have been used for modeling the drilled shaft in this study. Constraints include fixed supports for the bottom plane and roller supports for the plane in the x and y direction. A 7000 kips point load is applied at the top of the drilled shaft. In order to avoid high local compression of the drilled shaft due to point load, point load is distributed over the top surface of the drilled shaft. The Newton-Raphson method is an iterative process of solving the nonlinear equations which is used in this model

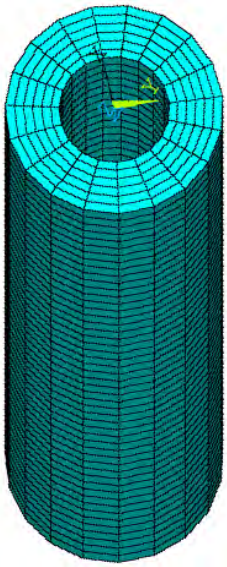

Figure 6: Meshing the Soil around the Shaft

Materials

The constructed model contains soil, concrete, and reinforcement bars. Table1 shows the material properties of the model.

Table 2: Material Properties

Material	Concrete	Steel Reinforcement
Elastic Modulus (ksi)	3,605	29,000
Poisson's Ratio	0.2	0.3

Drucker-Prager model is used with an approximation to the Mohr-Coulomb plasticity model but maintains the use of Cohesion and Dilatancy angle for the porous media. Von mises is used for the yield criterion and elastic-perfectly plastic for the material response of the Drucker-Prager model in ANSYS12. Table 3 shows the properties of the soil.

Table 3: Soil Properties

Modulus of Elasticity (ksi)	Poisson's ratio	Density (pcf)	Cohesion	Angle of friction	Dilatancy angle
13.88	0.45	120	0.06	35	30

The shaft is longitudinally reinforced with twenty nine No. 12 steel bars that are equally spaced around the perimeter. This amount of steel corresponds to 2.12 percent of the gross cross-sectional area of the shaft. The spirals consist of No. 8 bars spaced along the axis of the shafts at 20 in. Bi-linear stress-strain relationship is used for the steel (O'Neill and Reese (1999)) as shown in Figure 7(b). For steel, the value of yield stress (f_y) is the same in compression and in tension. Reinforcing steel used is Grade 60 with a yield stress of 60 ksi and a modulus (E) of 29,000 ksi.

Two different non-linear stress-strain relationships are also used for the concrete. The first one is unconfined stress-strain relationship and the second one is confined model. Concrete is used with 4000 psi ultimate compressive strength concrete. For concrete, the compressive strength depends on the mobilized compressive strain. Unconfined concrete model used in this study was

O'Neill and Reese model (1999) [7]. In this model, the compressive strength increases up to the reduced ultimate compressive strength (f_c''), which is taken as a percentage of the 28-day cylinder compressive strength. The strength in unconfined model is expressed as:

$$f_c = f_c''\left[2(\frac{\varepsilon}{\varepsilon_0}) - (\frac{\varepsilon}{\varepsilon_0})^2\right] \quad for \quad \varepsilon < \varepsilon_0 \tag{14}$$

$$f_c = 0.85 f_c'' \quad for \quad \varepsilon < 0.038$$

f_c = linearly interpolated for $\varepsilon_0 \leq \varepsilon \leq 0.038$

$$f_c'' = 0.85 f_c' \quad and \quad \varepsilon_0 = \frac{1.7 f_c'}{E_c} \tag{15}$$

where f'_c is the concrete compressive strength at 28 days, and E_c is the initial tangent slope of the stress-strain area. The value E_c can be estimated as:

$$E_c = 57000\sqrt{f_c'} \tag{16}$$

In such a case, a multilinear stress-strain relationship can be included which follows the stress-strain curve of the material being used. This will allow ANSYS to more accurately model the plastic deformation of the material. Confined concrete model used in this study was Mander model (1988) [7]. Reinforced concrete members with axial compression forces may be confined by using transverse steel to enhance the member strength and ductility. The form of the stress-strain curve for confined concrete can be expressed in terms of a simple uniaxial relationship.

Results

The results of the ANSYS model are shown in Figures 7 and 8. Figure 7 shows the displacement in Z direction on the drilled shaft nodes. It can be seen that vertical displacement at top of the shaft is around 2.4 inches and at the bottom of the shaft is 0.22 inches. Figure 8 shows displacement in Z direction on the stirrups and longitudinal bars nodes inside the shaft. The side resistance for the drilled shaft can be obtained by multiplying the stress in z-direction with the perimeter area of the shaft through the length of the drilled shaft. The tip resistance is calculated by multiplying the stress at the tip of the shaft with the area of the drilled shaft section. Results show that for this ANSYS model, 25 percent of the axial load is carried by the tip and 75 percent is resisted by the friction between soil and shaft.

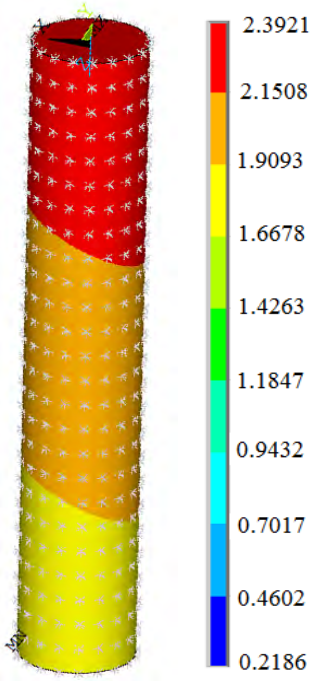

Figure 7: Z-component of Displacement in Drilled Shaft Nodes (Un-confined Model)

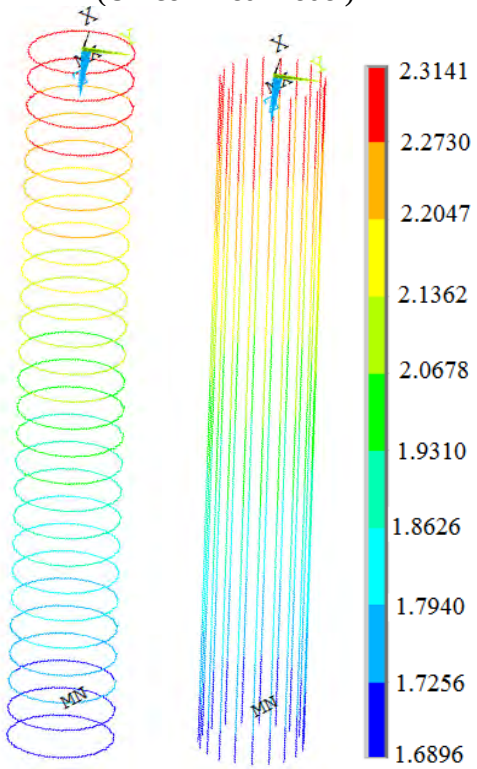

Figure 8: Z-component of Displacement in Longitudinal and Stirrups (Un-confined Model)

Figure 9 shows that load versus vertical displacement for the Finite Element model in the bottom, middle, and top node on the drilled shaft. It can be seen that they have almost the same

behavior as stress strain relationship. Also, Load versus vertical displacement in the soil nodes is shown in Figure 10 for three different nodes at the bottom, middle and top of the drilled shaft. It can be seen that there is a critical point load on the curve that vertical displacement decrease after that point. With increasing the axial load after 5000 kips, the vertical displacement on the soil nodes will decrease.

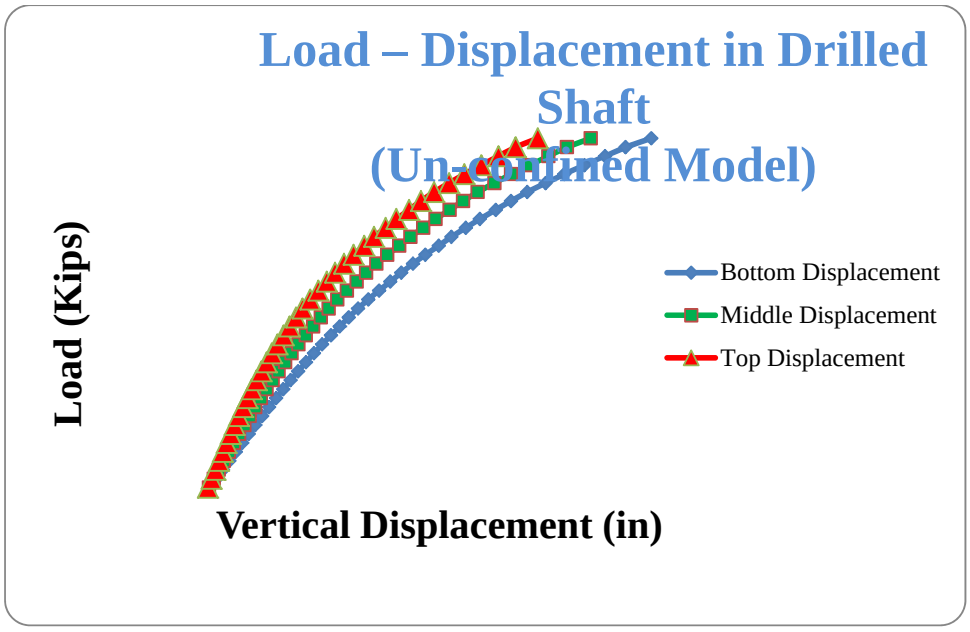

Figure 9: Load-displacement in drilled Shaft (Un-confined Model)

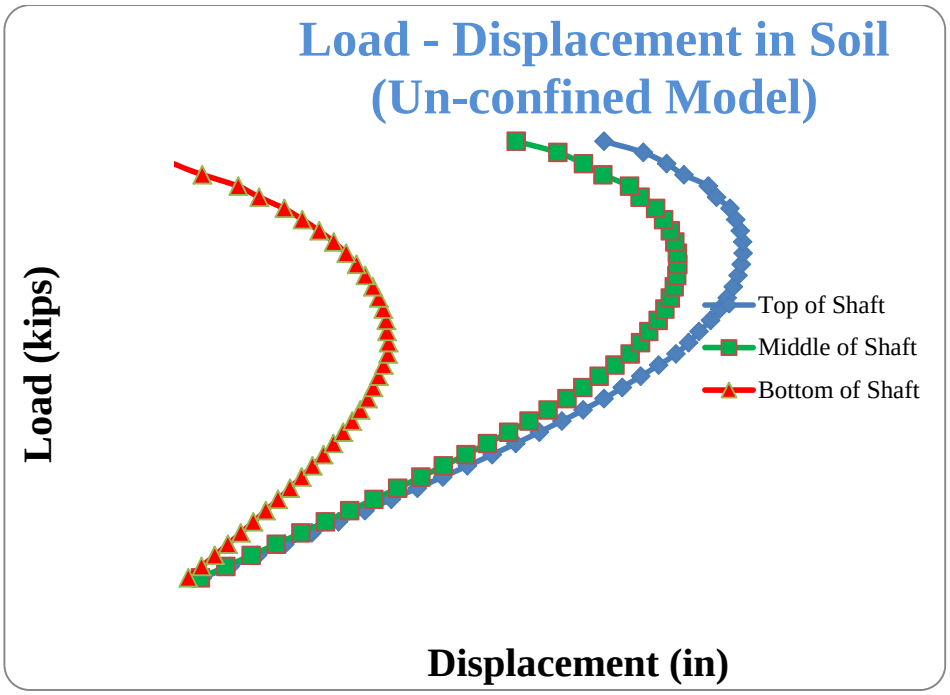

Figure 10: Load-displacement in Soil (Un-confined Model)

Here, we compare the analytical results with ANSYS results for both confined and un-confined models. It shows that un-confined model is closer to the analytical results since we have stirrup and longitudinal bars in the concrete and is closer to realistic. In confined model for the concrete, since bars have been removed and confined concrete model has been used for the stress-strain relationship, the load-displacement curve is less than analytical and unconfined results.

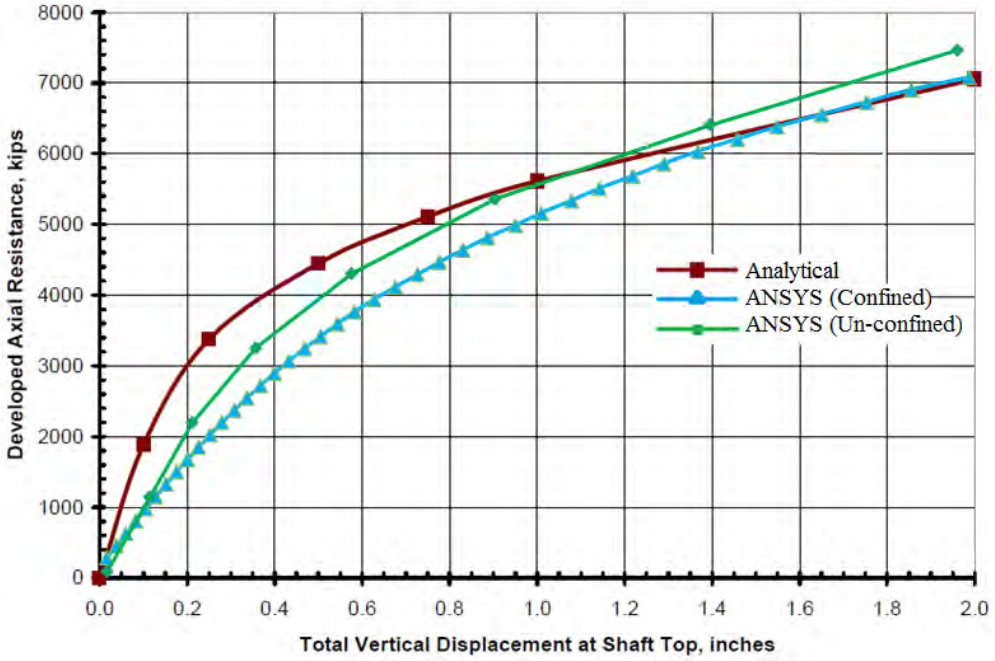

Figure 11: Load-displacement Analytical in Comparison to Finite Element

CONCLUSION

(1) A comprehensive finite element model for drilled shaft foundations was provided. This model can consider soil with different layers around the drilled shaft. It also can be run for drilled shafts with different diameters and lengths. Also, different type of concrete, confined model and unconfined model, and different type of soil can be used in the provided model.

(2) Based on the results presented, it is concluded that with increasing in the depth of the drilled shaft, side resistance percentage will be approximately increased on a second degree polynomial curve as shown in Figure 4.

(3) For drilled shafts with the diameters of 4 ft to 10 ft, in the first depths the difference between the total axial load capacities of drilled shafts is less than the end of the shafts.

(4) For a drilled shaft with 7 ft diameter, 95 ft length and soil profile shown in Table 1, both analytical and ANSYS model show that 75 percent of the total axial load is resisted by the soil around the shaft or side resistance and the rest of the axial load is resisted by the tip resistance.

(5) This study was primarily concerned about modeling a simple stress-strain relation for both unconfined and confined concrete which can represent the behavior of normal-

strength concrete in drilled shaft foundations. This study considered two different models for the concrete, confined and unconfined model. Results show that un-confined concrete model had closer results to the analytical results in comparison to confined concrete model.

REFERENCES

1. Reese, L. C., O'Neill, M. W. (1999). "Drilled Shafts: Construction Procedures and Design Methods," Publication No. FHWA-IF-99-025, Federal Highway Administration.
2. AASHTO. 2002. Standard Specifications for Highway Bridges, 17th Edition, HB-17. American Association of State Highway and Transportation Officials, Washington, DC.
3. Rollins, K. M., Clayton, R. J., Mikesell, R. C., Blaise, B. C. (2005). "Drilled Shaft Side Friction in Gravelly Soil." Journal of Geotechnical and Geoenvironmetral Engineering, Volume 131, Issue 8, 987-1003.
4. Bal Krishna Maheshwari, Kevin Z. Truman, M. Hesham El Naggar, and Phillip L. Gould, Three dimensional finite element nonlinear dynamic analysis of pile groups for lateral transient and seismic excitations, NRC Research Press, Can. Geotech. J. 41: 118–133 (2004)
5. Bathe, K.J. 1982. Finite element procedures in engineering analysis. Prentice-Hall, Inc., Englewood Cliffs, N.J.
6. Geotechnical Design Policy DS-1 , Intermodal Transportation Division, 206 South Seventeenth Avenue Phoenix, Arizona 85007-3213, Arizona Department of Transportation, December 2010, page14.
7. Reddier M. K. M., (2009). "Stress-Strain Model of Unconfined and Confined Concrete and Stress-Block Parameters." Master Thesis, Texas A&M University.
8. Sahadat Hossain, Victor Omelchenko, Mohammed Adil Haque, Jubair Hossain, Capacity of a Drilled Shaft in Mid-Atlantic Region, EJGE, Vol. 13, Bund. E.
9. Yang, M. Z., Islam, M. Z., Drumm, E. C., Zuo, G. (2004). "Side Resistance of Drilled Shaft Socketed into Wissahickon Mica Schist." Geotechnical Special Publication, No. 124, GeoSupport 2004 – Drilled Shafts, Micropiling, Deep Mixing, Remedial Methods, and Specialty Foundation Systems, Proceedings of Sessions of the GeoSupport Conference: Innovation and Cooperation in Geo, 765-777.